Chapter 1

Modeling 3D Movements with the Kinematic Theory of Rapid Human Movements

Andreas Fischer[⋆†], Roman Schindler[⋆], Manuel Bouillon[⋆] and Réjean Plamondon[‡]

[⋆]*DIVA Group, University of Fribourg, Switzerland*
[†]*iCoSys Institute, HES-SO Fribourg, Switzerland*
[‡]*Laboratoire Scribens, Polytechnique Montréal, Canada*
{andreas.fischer,roman.schindler,manuel.bouillon}@unifr.ch,
rejean.plamondon@polymtl.ca

The Kinematic Theory of rapid human movements analytically describes pen tip movements as a sequence of elementary strokes with lognormal speed. The theory has been confirmed in a large number of experimental evaluations, achieving a high reconstruction quality when compared with observed trajectories and providing pertinent features for biomedical applications as well as biometric identification. So far, the Kinematic Theory has focused on one-dimensional movements with the Delta-Lognormal model and on two-dimensional movements with the Sigma-Lognormal model. In this chapter, we present a model for movements in three dimensions, which naturally extends the Sigma-Lognormal approach. We evaluate our method on two action recognition datasets and an air-writing dataset, demonstrating a high reconstruction quality for modelling rapid 3D movements in all cases.

1. Introduction

The Kinematic Theory of rapid human movements [Plamondon, 1995a,b, 1998, Plamondon *et al.*, 2003] is one of the most comprehensive theories on the production process of handwriting. It postulates that pen tip movements are the result of a series of elementary neuromuscular strokes, whose speed is a lognormal function. When compared with other frameworks for human movement modeling, such as coupled oscillator models [Hollerbach, 1981] or minimum jerk models [Flash and Hogans, 1985], the Kinematic Theory stands out with an excellent reconstruction quality of observed trajectories [Plamondon *et al.*, 1993], i.e. the analytical representation is highly accurate.

Moreover, an increasing number of experiments suggest that the analytical representation provided by the Kinematic Theory indeed captures neuromuscular properties of the writer, which can be exploited for the analysis of human motor control. Successful applications include learning tools for children [Djeziri *et al.*, 2002, Rémi *et al.*, 2017], biomedical applications [Plamondon *et al.*, 2013, O'Reilly *et al.*, 2014], gesture recognition [Almaksour *et al.*, 2011], handwriting recognition [Fischer *et al.*, 2014, Martin-Albo *et al.*, 2014], and signature verification [Galbally *et al.*, 2012a,b, Diaz *et al.*, 2018, Fischer and Plamondon, 2017], to name just a few. Besides the analysis of finger movements, the Kinematic Theory has also been applied to analyze wrist, arm, head, and eye movements [Plamondon, 1995a], and recently on head trunk rotations [Lebel *et al.*, 2017] as well as for speech processing [Carmona-Duarte *et al.*, 2016].

Except for a few published and unpublished exploratory studies [Leduc and Plamondon, 2001, Djioua, 2007], the Kinematic Theory has focused on movements in one and two dimensions. Rapid 1D movements are modeled by two opposed neuromuscular systems generating agonist and antagonist movements, according to the Delta-Lognormal model ($\Delta\Lambda$) [Plamondon and Guerfali, 1998]. Complex 2D movements, such as signatures, are modeled by a vectorial sum of strokes, i.e. several movements that are overlapping in time during execution, according to the Sigma-Lognormal model ($\Sigma\Lambda$) [Plamondon and Djioua, 2006].

In both cases, algorithms are needed to extract the model parameters from observed trajectories. The Robust XZERO algorithm [Djioua and Plamondon, 2008] has been proposed to estimate the parameters of the $\Delta\Lambda$ model from the velocity profile. For estimating the parameters of the $\Sigma\Lambda$ model, the Robust XZERO algorithm is complemented with an estimation of the start and end angles of the two-dimensional strokes [O'Reilly and Plamondon, 2009]. Improved variants of this approach include a breadth-first search strategy that minimizes the number of strokes [Martin-Albo *et al.*, 2015] and the recently introduced iDeLog method [Ferrer *et al.*, 2018], which estimates the lognormal parameters not only from the velocity profile but also from the trace, taking into account visual feedback.

In this chapter, we present a three-dimensional model for the Kinematic Theory. It naturally extends the $\Sigma\Lambda$ model by introducing an additional angle for the third dimension. The present chapter builds upon our recent conference paper [Schindler *et al.*, 2018], which has introduced the method. Additional contributions include a more comprehensive description of the 3D model as well as an extended experimental evaluation on two supplementary motion datasets. In our experiments, we measure the reconstruction quality of the 3D model in terms of signal-to-noise-ratio (SNR) as well as classification accuracy on two action recognition datasets, namely HDM05 [Müller *et al.*, 2007] and UTKinect [Xia *et al.*, 2012], as well as an air-writing dataset [Chen *et al.*, 2016]. While the air-writing dataset consists of finger movements, the action recognition datasets are based on wrist and ankle movements.

The remainder of this chapter is organized as follows. Section 2 reviews the standard $\Sigma\Lambda$ model of the Kinematic Theory, Section 3 details our proposed extension to three dimensions, and Section 4 reports experimental results. Finally, we draw conclusions in Section 5 and discuss future lines of research for modeling 3D movements with the Kinematic Theory.

2. Sigma-Lognormal Model

The Sigma-Lognormal model ($\Sigma\Lambda$) [Plamondon and Djioua, 2006] of the Kinematic Theory represents a two-dimensional pen tip movement as a series of elementary *strokes*.[a] An individual stroke is initiated at time t_0 in the central nervous system to cover distance D. It is then executed with lognormal speed

$$|\vec{v}(t)| = \frac{D}{\sqrt{2\pi} \cdot \sigma(t - t_0)} \exp\left(-\frac{[\ln(t - t_0) - \mu]^2}{2\sigma^2}\right) \quad , \tag{1}$$

where μ is the log time delay and σ is the log response time, which depend on the neuromuscular system. The distance traveled at time t is

$$d(t) = \int_0^t |\vec{v}(\tau)| d\tau = \frac{D}{2}\left[1 + \text{erf}\left(\frac{\ln(t - t_0) - \mu}{\sigma\sqrt{2}}\right)\right] \quad . \tag{2}$$

The $\Sigma\Lambda$ model assumes that each 2D stroke follows a circular trajectory with start angle θ_s and end angle θ_e. The angular position is

$$\theta(t) = \theta_s + (\theta_e - \theta_s)\frac{d(t)}{D} \quad . \tag{3}$$

To sum up, each lognormal stroke s is characterized by a total of six parameters

$$s = (t_0, D, \mu, \sigma, \theta_s, \theta_e) \quad . \tag{4}$$

[a] Note that the term *stroke* is sometimes used to describe the pen tip movement between pen-down and pen-up. In the present context of kinematic analysis, it refers to a movement primitive described by a lognormal velocity profile. [Woch and Plamondon, 2004].

Finally, the velocity of the 2D movement is given by vectorial summation of n individual strokes

$$\vec{v}(t) = \sum_{i=1}^{n} \vec{v_i}(t) \quad . \tag{5}$$

The underlying assumption is that the strokes are scheduled in an action plan according to their initiation time t_0 and overlap in their execution.

For reconstructing the velocity and the trace of a 2D pen tip movement based on the analytical $\Sigma\Lambda$ representation, it follows that

$$v_x(t) = \sum_{i=1}^{n} |\vec{v_i}(t)| \cos(\theta_i(t)) \quad , \tag{6}$$

$$v_y(t) = \sum_{i=1}^{n} |\vec{v_i}(t)| \sin(\theta_i(t)) \quad , \tag{7}$$

$$x(t) = \int_0^t v_x(\tau) d\tau \quad , \tag{8}$$

$$y(t) = \int_0^t v_y(\tau) d\tau \quad . \tag{9}$$

Figure 1 illustrates a handwritten signature and its $\Sigma\Lambda$ model. The observed as well as the reconstructed signature is shown, together with the circular trajectories of the individual strokes. The signal-to-noise ratio (SNR) is 27dB for this example, which is highly accurate (see Section 2.2).

For more details, we refer to the articles that introduce the Kinematic Theory. [Plamondon, 1995a,b, 1998, Plamondon *et al.*, 2003].

2.1. *Stroke Extraction and Parameter Estimation*

One of the most widely used algorithms for stroke extraction and estimation of the $\Sigma\Lambda$ parameters is based on an iterative detection of strokes in the velocity profile [O'Reilly and Plamondon, 2009].

In order to improve the stability of the algorithm, certain signal preprocessing steps are recommended. First, it can be helpful to stop the pen tip artificially at the beginning and at the end of the movement during $200ms$, to ensure zero velocity. Secondly, if the acquisition device has a low or unstable sampling rate, an interpolation of the velocity profile with cubic splines and a resampling at $200Hz$ is suggested. Finally, a low-pass filter can be used to remove noise introduced by the acquisition device.

After preprocessing, strokes are extracted iteratively from the signal. The following five steps describe the extraction of a single stroke:

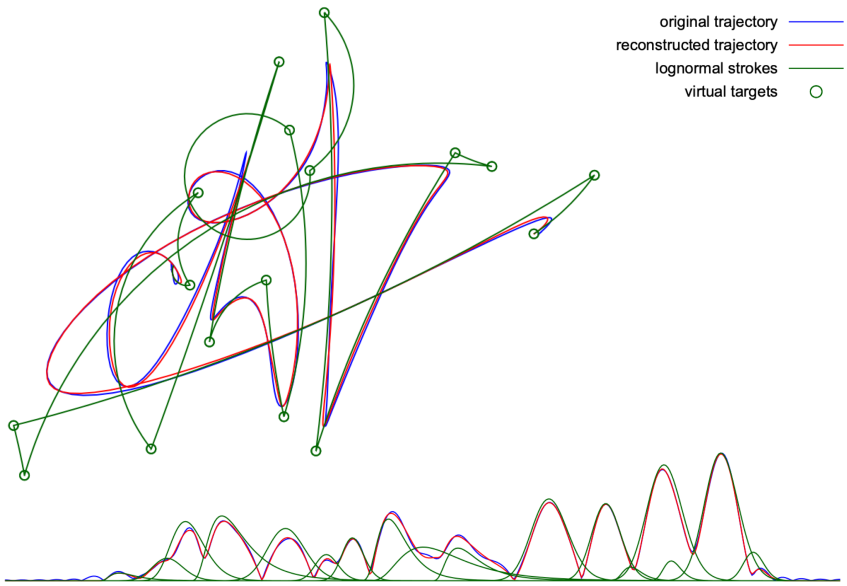

Fig. 1. Sigma-Lognormal reconstruction of the trace and the velocity profile of a handwritten signature [Fischer and Plamondon, 2017].

(1) Detect new stroke in the speed profile $|\vec{v}(t)|$.
(2) Estimate parameters D, t_0, μ, and σ.
(3) Estimate angular parameters θ_s and θ_e.
(4) Optimize parameter estimation.
(5) Remove stroke from the speed profile.

These steps are repeated until there are no more strokes detected in the speed profile.

Step 1 detects a local maximum in the speed profile together with neighboring infexion points and minima. The maximum speed and the area under curve have to exceed a minimum value.

Step 2 applies the Robust XZERO algorithm [Djioua and Plamondon, 2008] to estimate the speed-related parameters D, t_0, μ, and σ. It is based on zero crossings of the first and second derivatives of the lognormal function.

Step 3 estimates the start angle θ_s and the end angle θ_e based on five characteristic times of the lognormal stroke illustrated in Figure 2. The start and end are chosen as $t_1 = t_0 + \exp(\mu - 3\sigma)$ and $t_5 = t_0 + \exp(\mu + 3\sigma)$,

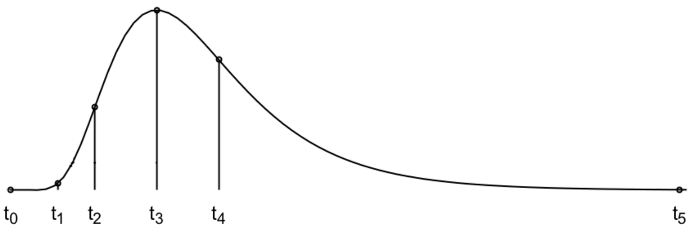

Fig. 2. Characteristic times of a lognormal stroke.

respectively. The maximum speed is reached at $t_3 = t_0 + \exp(\mu - \sigma^2)$, and the inflection points are $t_2 = t_0 + \exp(\mu - 1.5\sigma^2 - \sigma\sqrt{0.25\sigma^2 + 1})$ and $t_4 = t_0 + \exp(\mu - 1.5\sigma^2 + \sigma\sqrt{0.25\sigma^2 + 1})$, respectively.

The angular parameters are obtained by means of linear extrapolation. Considering the velocity angle

$$\theta(t) = \arctan \frac{v_y(t)}{v_x(t)} \quad , \tag{10}$$

the angular derivative is calculated with respect to the distance traveled at time t_4 and t_2 (see Equation 2)

$$\Delta\theta = \frac{\theta(t_4) - \theta(t_2)}{d(t_4) - d(t_2)} \quad . \tag{11}$$

Finally, the start and end angles are estimated using

$$\hat{\theta}_s = \theta(t_3) - (d(t_3) - d(t_1))\Delta\theta \quad , \tag{12}$$

$$\hat{\theta}_e = \theta(t_3) + (d(t_5) - d(t_3))\Delta\theta \quad . \tag{13}$$

Step 4 optimizes the initial parameter estimation using non-linear least squares curve fitting.

Step 5 removes the new stroke from the speed profile before the next stroke is detected.

For more details on stroke extraction and parameter estimation, we refer to the original article [O'Reilly and Plamondon, 2009].

2.2. *Model Quality*

The analytical $\Sigma\Lambda$ model allows to reconstruct the movement using Equations 6-9. The quality of the model can be evaluated by means of a signal-to-noise ratio (SNR) between the observed velocity $\vec{v}_o(t)$ and the reconstructed velocity $\vec{v}_r(t)$. With respect to the start time t_s and end time t_e

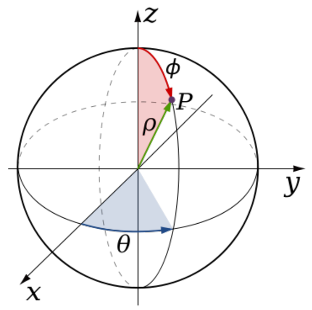

Fig. 3. Spherical coordinates of the 3D model.

of the movement, the SNR is

$$SNR = 10 \cdot \log \left(\frac{\int_{t_s}^{t_e} |\vec{v}_o(\tau)|^2 d\tau}{\int_{t_s}^{t_e} |\vec{v}_o(\tau) - \vec{v}_r(\tau)|^2 d\tau} \right) \quad . \tag{14}$$

In practice, we approximate the integral with the trapezoidal rule over all sampling points.

3. 3D Model Extension

The proposed 3D model naturally extends the $\Sigma\Lambda$ model by introducing an additional angle $\phi(t)$ for the third dimension as illustrated in Figure 3, where the radius $\rho = |\vec{v}(t)|$ corresponds to the speed.

Assuming that strokes act along a pivot direction, we model the new angle similar to Equation 3 by

$$\phi(t) = \phi_s + (\phi_e - \phi_s) \frac{d(t)}{D} \quad . \tag{15}$$

That is, the change in the angle is proportional to the distance traveled.

Two additional parameters are thus introduced to the stroke model, i.e. the start angle ϕ_s and the end angle ϕ_e in the third dimension

$$s_{3D} = (t_0, D, \mu, \sigma, \theta_s, \theta_e, \phi_s, \phi_e) \quad . \tag{16}$$

For reconstructing the velocity based on the 3D model, Equations 6 and 7 have to be modified. The three velocity components are

$$v_x(t) = \sum_{i=1}^{n} |\vec{v}_i(t)| \sin(\phi_i(t)) \cos(\theta_i(t)) \quad , \tag{17}$$

$$v_y(t) = \sum_{i=1}^{n} |\vec{v}_i(t)| \sin(\phi_i(t)) \sin(\theta_i(t)) \quad , \tag{18}$$

$$v_z(t) = \sum_{i=1}^{n} |\vec{v}_i(t)| \cos(\phi_i(t)) \quad . \tag{19}$$

For reconstructing the position, Equations 8 and 9 remain the same. The three position components are

$$x(t) = \int_0^t v_x(\tau) d\tau \quad , \tag{20}$$

$$y(t) = \int_0^t v_y(\tau) d\tau \quad , \tag{21}$$

$$z(t) = \int_0^t v_z(\tau) d\tau \quad . \tag{22}$$

The stroke extraction and parameter estimation procedure follows the same procedure as in 2D (see Section 2.1). In Step 3, the additional angles ϕ_s and ϕ_e are estimated similar to θ_s and θ_e.

Considering the velocity angle

$$\theta(t) = \arccos \frac{v_z(t)}{\rho} \quad , \tag{23}$$

where $\rho = |\vec{v}(t)|$ is the speed, we estimate the new angles similar to Equations 11-13:

$$\Delta\phi = \frac{\phi(t_4) - \phi(t_2)}{d(t_4) - d(t_2)} \quad , \tag{24}$$

$$\hat{\phi}_s = \phi(t_3) - (d(t_3) - d(t_1))\Delta\phi \quad , \tag{25}$$

$$\hat{\phi}_e = \phi(t_3) + (d(t_5) - d(t_3))\Delta\phi \quad . \tag{26}$$

The proposed modifications of the $\Sigma\Lambda$ model allow us to extract 3D strokes from any three-dimensional movement. By vectorial summation of the strokes, the analytical model enables us to reconstruct the movement. The model quality is measured in terms of SNR as described in Section 2.2.

4. Experimental Evaluation

The proposed 3D model has been evaluated on three publicly available motion datasets described in Section 4.1. Besides reporting the SNR in Section 4.2, we also investigate the reconstructed 3D movements in the context of a classification experiment in Section 4.3.

Table 1. 3D motion datasets.

	HDM05	UTKinect	Air-Writing
Type of activities	Actions	Actions	Words
Number of subjects	5	10	5
Number of classes	11	10	100
Number of samples	249	199	500
Acquisition device	Vicon	Kinect	Leap
Sampling rate	120 Hz	15 Hz	60 Hz

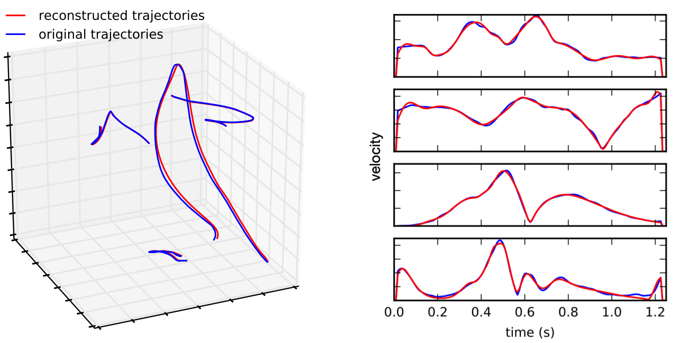

Fig. 4. Original (blue) and reconstructed (red) traces and velocity profiles of the four limbs for a kick action from the HDM05 dataset.

4.1. *Datasets*

A summary of the motion datasets is provided in Table 1, including the number of subjects who performed 3D movements, the number of classes (types of movements), the total number of samples in the dataset, the acquisition device, and the sampling rate.

Exemplary 3D trajectories together with their reconstructions are shown in Figures 4-6 for each of the datasets.

HDM05. The HDM05 dataset [Müller *et al.*, 2007] contains around 1500 motion samples of 100 different action classes, performed by five subjects. The movements were recorded with an optical marker-based motion capture suit of Vicon with a sampling rate of 120 Hz.

We use a common subset of eleven classes and 249 samples. The classes are *deposit floor*, *elbow to knee*, *grab high*, *hop both legs*, *jog*, *kick forward*,

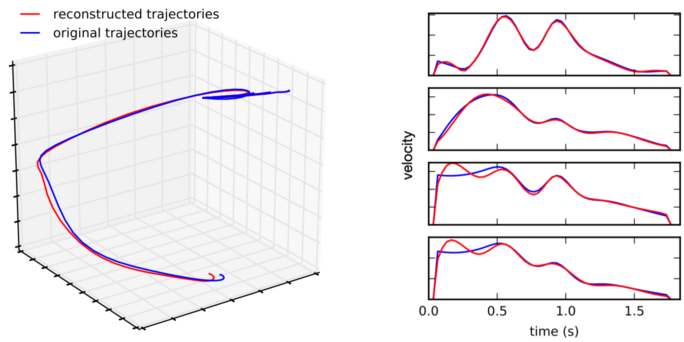

Fig. 5. Original (blue) and reconstructed (red) traces and velocity profiles of the four limbs for a throwing action from the UTKinect dataset.

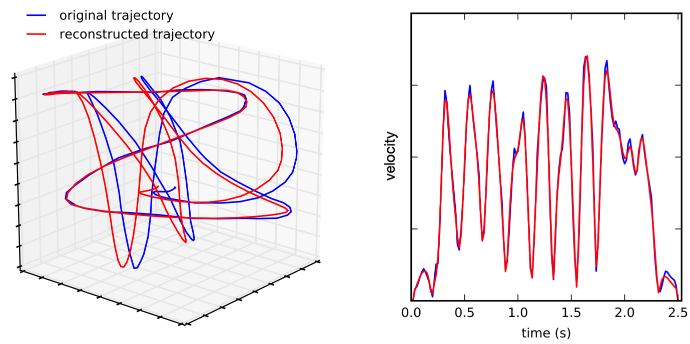

Fig. 6. Original (blue) and reconstructed (red) traces and velocity profiles of the fingertip for the word *ZIP* from the Air-Writing dataset.

lie down floor, *rotate both arms backward*, *sneak*, *squat* and *throw basketball*.

Four 3D trajectories are considered for our experiments, namely the wrists relative to the shoulders and the ankles relative to the hips [Boulahia *et al.*, 2016]. These trajectories are then normalized by the length of arms and legs of the subject, which supports action recognition across different persons [Kulpa *et al.*, 2005].

UTKinect. The UTKinect dataset [Xia *et al.*, 2012] is composed of 199 samples of 10 actions performed by 10 subjects. The movements are recorded by a Kinect camera with a sampling rate of 30Hz. However, frames were only recorded when the skeleton was tracked, causing missing

Table 2. Reconstruction quality in terms of SNR.

	HDM05		UTKinect		Air-Writing	
	2D	3D	2D	3D	2D	3D
Mean	19.19	18.52	21.87	20.21	12.60	12.52
Standard deviation	3.77	4.09	3.62	4.40	2.02	2.02

frames and a final sampling rate of about 15Hz.

Ten indoor activities include *walk*, *sit down*, *stand up*, *pick up*, *carry*, *throw*, *push*, *pull*, *wave* and *clap hands*.

Similar to the HDM05 dataset, we consider four 3D trajectories of normalized wrist and ankle movements.

Air-Writing. The Air-Writing dataset [Chen *et al.*, 2016] includes 150 short words written with the index finger into the air by 18 subjects. They consist of uppercase letters A-Z and were written with a specified movement order in box-writing style, i.e. on top of each other. The writing is recorded without markers or gloves using a Leap camera with a sampling rate of 60Hz.

For our experiments, we consider 100 common words written by 5 subjects (C3, J1, M3, T3, W1), resulting in a total of 500 fingertip trajectories.

4.2. *SNR Results*

Table 2 reports the mean SNR of our 3D model together with the standard deviation for all three datasets. It is compared with the SNR achieved with the unmodified $\Sigma\Lambda$ model when the z-direction is disregarded. Detailed bar plots are provided in Figure 7.

Despite the increased complexity of modeling 3D movements, the proposed method achieves a high model quality that is only slightly below the 2D results. Actions recorded by the Vicon suit (HDM05) and the Kinect camera (UTKinect) have a significantly higher SNR than the finger movement recorded with the Leap camera (Air-Writing), which may be due to the larger scale of the whole-body actions when compared with the relatively small finger movements. In all three datasets, the movements are rather rapid with a duration of less than five seconds on average.

These results also demonstrate that the proposed algorithm can work with low frequency sampled signals as compared to most of the previous studies where the sampling frequency is above 100 Hz, generally 200Hz.

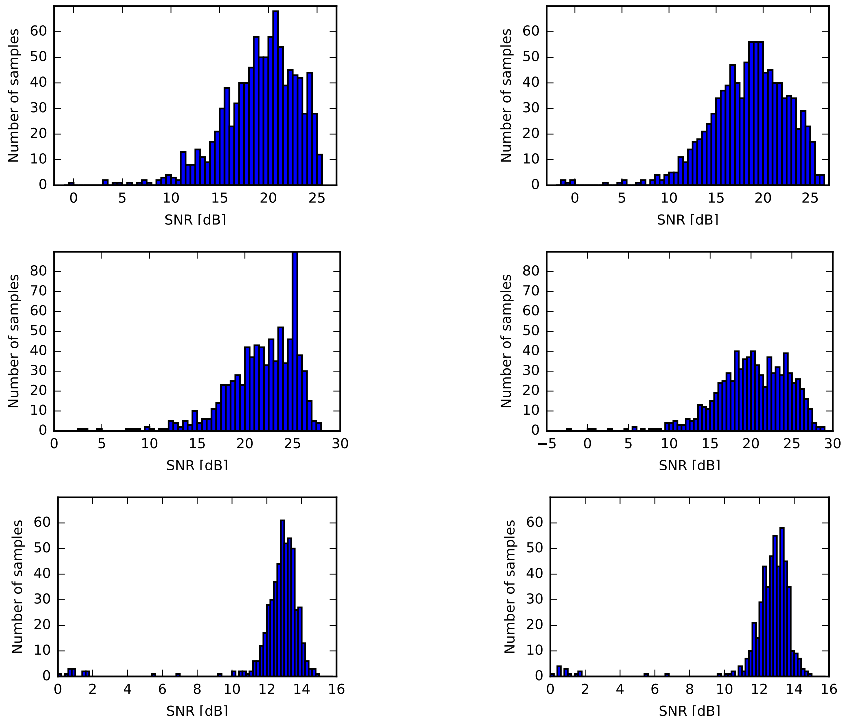

Fig. 7. SNR histograms for 2D reconstructions (left) and 3D reconstructions (right) of the HDM05, UTKinect, and Air-Writing datasets (top to bottom).

4.3. *Classification Results*

In a final experiment, we have classified the different types of movements using dynamic time warping (DTW) [Schindler *et al.*, 2018].

During preprocessing, we resample the original trajectories at 30Hz for HDM05 and at 15Hz for UTKinect and Air-Writing using cubic spline interpolation, in order to obtain a stable sampling rate and to speedup the DTW computation. The reconstructed trajectories are computed at the same sampling times. Afterwards, we use a second-order regression to compute velocity and acceleration as additional features leading to a total of nine features $(x, y, z, v_x, v_y, v_z, a_x, a_y, a_z)$ per sample point.

The classifier is optimized for each dataset separately with respect to feature selection and feature normalization. For HDM05, the best results are achieved when considering only the velocity for each of the four limbs, normalized to zero mean and unit variance for each movement. For UTKinect, only the position is considered for each of the four limbs and no normalization is applied. For Air-Writing, position and velocity are considered for the finger movement, normalized to zero mean.

For classification, the DTW distance is computed for all pairs of movements. Each movement is then assigned to the same class as the nearest neighbor in the dataset performed by other subjects. In order to speedup the distance computation and to avoid unrealistic warping paths, we use DTW with a Sakoe-Chiba band of width $|n_1 - n_2| + 10$, where n_1 and n_2 are the number of sampling points of the two movements. The resulting DTW distance is normalized with the total number of sampling points $n_1 + n_2$.

The classification results are reported in Table 3 both for original and reconstructed samples, respectively. In all cases, we observe only a slight deviation in the classification accuracy, which emphasizes the high quality of the proposed 3D model.

Table 3. Classification accuracy using original and reconstructed 3D movements.

	Original	Reconstructed
HDM05	96.4	96.1
UTKinect	94.0	92.0
Air-Writing	99.0	98.2

5. Conclusions

The proposed 3D model of the Kinematic Theory of rapid human movements has demonstrated a high reconstruction quality for rapid 3D movements of ankles, wrists, and fingertips recorded with diverse equipment.

There are several promising lines of future research to pursue. First, there seems to be potential to improve the current stroke extraction and parameter estimation method, for example by minimizing the number of strokes [Martin-Albo *et al.*, 2015] or by taking into account visual feedback [Ferrer *et al.*, 2018]. Secondly, the synthesis of 3D movements may be highly rewarding. It can support classifiers with realistic training data. Thirdly, there is a wide range of new applications that may emerge from modelling 3D motions with the Kinematic Theory in biomedicine, biometrics, and robotics.

From a more fundamental perspective, our results support the universality of the lognormality principle and its potential use to study any kind of human movements.

References

Almaksour, A., Anquetil, E., Plamondon, R. and O'Reilly, C. (2011). Synthetic handwritten gesture generation using sigma-logormal model for evolving handwriting classifier, in *Proc. 15th Int. Conf. of the International Graphonomics Society*, pp. 98–101.

Boulahia, S. Y., Anquetil, É., Kulpa, R. and Multon, F. (2016). HIF3D: handwriting-inspired features for 3d skeleton-based action recognition, in *23rd International Conference on Pattern Recognition, ICPR 2016, Cancún, Mexico, December 4-8, 2016*, pp. 985–990.

Carmona-Duarte, C., Plamondon, R., Gomez-Vilda, P., Ferrer, M., Alonso, J. and Londral, A. R. M. (2016). Application of the lognormal model to the vocal tract movement to detect neurological diseases in voice, *Innovation in Medicine and Healthcare* **60**, pp. 25–35.

Chen, M., AlRegib, G. and Juang, B.-H. (2016). Air-writing recognition – part ii: Detection and recognition of writing activity in continuous stream of motion data, *IEEE Trans. on Human-Machine Systems* **46**, 3, pp. 436–444.

Diaz, M., Fischer, A., Ferrer, M. and Plamondon, R. (2018). Dynamic signature verification system based on one real signature, *IEEE Trans. on Cybernetics* **48**, 1, pp. 228–239.

Djeziri, S., Guerfali, W., Plamondon, R. and Robert, J. (2002). Learning handwriting with pen-based systems: computational issues, *Pattern Recognition* **35**, 5, pp. 1049–1057.

Djioua, M. (2007). *Contributions à la compréhension, à la généralisation et à l'application de la Théorie Cinématique dans l'analyse et la synthèse du mouvement humain*, Ph.D. thesis, Polytechnique Montréal.

Djioua, M. and Plamondon, R. (2008). A new algorithm and system for the extraction of delta-lognormal parameters, Tech. Rep. EPM-RT-2008-04, École Polytechnique de Montréal.

Ferrer, M., Diaz, M., Carmona, C. and Plamondon, R. (2018). iDeLog: Iterative dual spatial and kinematic extraction of sigma-lognormal parameters, *IEEE Trans. PAMI* **PP**, pp. 1–12.

Fischer, A. and Plamondon, R. (2017). Signature verification based on the kinematic theory of rapid human movements, *IEEE Trans. on Human-Machine Systems* **47**, 2, pp. 169–180.

Fischer, A., Plamondon, R., O'Reilly, C. and Savaria, Y. (2014). Neuromuscular representation and synthetic generation of handwritten whiteboard notes, in *Proc. 14th Int. Conf. on Frontiers in Handwriting Recognition*, pp. 222–227.

Flash, T. and Hogans, N. (1985). The coordination of arm movements: An experimentally confirmed mathematical model, *Journal of Neuroscience* **5**, pp. 1688–1703.

Galbally, J., Plamondon, R., Fierrez, J. and Ortega-Garcia, J. (2012a). Synthetic on-line signature generation. Part I: Methodology and algorithms, *Pattern Recognition* **45**, 7, pp. 2610–2621.

Galbally, J., Plamondon, R., Fierrez, J. and Ortega-Garcia, J. (2012b). Synthetic on-line signature generation. Part II: Experimental validation, *Pattern Recognition* **45**, 7, pp. 2622–2632.

Hollerbach, J. (1981). An oscillation theory of handwriting, *Biological Cybernetics* **39**, 2, pp. 139–156.

Kulpa, R., Multon, F. and Arnaldi, B. (2005). Morphology-independent representation of motions for interactive human-like animation, in *Eurographics*.

Lebel, K., Nguyen, H., Duval, C., Plamondon, R. and Boissy, P. (2017). Capturing the cranio-caudal signature of a turn with inertial measurement systems: Methods, parameters robustness and reliability, *Frontiers in Bioengineering and Biotechnology* **5**, 51, pp. 1–13.

Leduc, N. and Plamondon, R. (2001). A new approach to study human movements: The three dimensional delta-lognormal model, in *Proc. 10th Conf. of the International Graphonomics Society*, pp. 98–102.

Martin-Albo, D., Plamondon, R. and Vidal, E. (2014). Training of on-line handwriting text recognizers with synthetic text generated using the kinematic theory of rapid human movements, in *Proc. 14th Int. Conf. on Frontiers in Handwriting Recognition*, pp. 543–548.

Martin-Albo, D., Plamondon, R. and Vidal, E. (2015). Improving sigma-lognormal parameter extraction, in *Proc. 13th Int. Conf. on Document Analysis and Recognition*, pp. 286–290.

Müller, M., Röder, T., Clausen, M., Eberhardt, B., Krüger, B. and Weber, A. (2007). Documentation mocap database HDM05, Tech. Rep. CG-2007-2, Universität Bonn.

O'Reilly, C. and Plamondon, R. (2009). Development of a sigma-lognormal representation for on-line signatures, *Pattern Recognition* **42**, 12, pp. 3324–3337.

O'Reilly, C., Plamondon, R. and Lebrun, L.-H. (2014). Linking brain stroke risk factors to human movement features for the development of preventive tools, *Frontiers in Aging Neuroscience* **6**.

Plamondon, R. (1995a). A kinematic theory of rapid human movements. I. movement representation and generation, *Biological Cybernetics* **72**, 4, pp. 295–307.

Plamondon, R. (1995b). A kinematic theory of rapid human movements. II. movement time and control, *Biological Cybernetics* **72**, 4, pp. 309–320.

Plamondon, R. (1998). A kinematic theory of rapid human movements: III. kinetic outcomes, *Biological Cybernetics* **78**, 2, pp. 133–145.

Plamondon, R., Alimi, A., Yergeau, P. and Leclerc, F. (1993). Modelling velocity profiles of rapid movements: a comparative study, *Biological Cybernetics* **69**, 2, pp. 119–128.

Plamondon, R. and Djioua, M. (2006). A multi-level representation paradigm for handwriting stroke generation, *Human Movement Science* **25**, 4–5, pp. 586–607.

Plamondon, R., Feng, C. and Woch, A. (2003). A kinematic theory of rapid human movements: IV: A formal mathematical proof and new insights, *Biological Cybernetics* **89**, 2, pp. 126–138.

Plamondon, R. and Guerfali, W. (1998). The generation of handwriting with delta–lognormal synergies, *Biological Cybernetics* **78**, pp. 119–132.

Plamondon, R., O'Reilly, C., Rémi, C. and Duval, T. (2013). The lognormal handwriter: learning, performing, and declining, *Frontiers in Psychology* **4**, 945.

Rémi, C., Nagau, J., Vaillant, J. and Plamondon, R. (2017). Preliminary study of t0, a sigma-lognormal parameter extracted from young children's controlled scribbles, in *Proc. 18th Conf. of the International Graphonomics Society*, pp. 109–113.

Schindler, R., Bouillon, M., Plamondon, R. and Fischer, A. (2018). Extending the sigma-lognormal model of the kinematic theory to three dimensions, in *Proc. 1st Int. Conf. on Pattern Recognition and Artificial Intelligence*, pp. 748–752.

Woch, A. and Plamondon, R. (2004). Using the framework of the kinematic theory for the definition of a movement primitive, *Motor Control* **8**, 4, pp. 547–557.

Xia, L., Chen, C. and Aggarwal, J. (2012). View invariant human action recognition using histograms of 3d joints, in *Proc. IEEE Conf. on Computer Vision and Pattern Recognition Workshops (CVPRW)*, pp. 20–27.